Research Square

Preprints are preliminary reports that have not undergone peer review.
They should not be considered conclusive, used to inform clinical practice,
or referenced by the media as validated information.

Efficacy of computer-aided navigation in achieving mandibular contour symmetry during bimaxillary orthognathic surgery

Ningning Sun
Affiliated Hospital of Qingdao University
Jian Sun
Affiliated Hospital of Qingdao University
Zexian Xu
Affiliated Hospital of Qingdao University
Yanshan Liu
Affiliated Hospital of Qingdao University
Yupeng Wu
Affiliated Hospital of Qingdao University
Ming Sun
Affiliated Hospital of Qingdao University
Qian Yang
Affiliated Hospital of Qingdao University
Yang Liu
Affiliated Hospital of Qingdao University
Chen Chen
pkuss2009@163.com

Affiliated Hospital of Qingdao University

Research Article

Keywords: Computer-aided navigation, Orthognathic surgery, Mandibular contouring, Mandibular symmetry, Facial aesthetics

Posted Date: July 31st, 2026

DOI: https://doi.org/10.21203/rs.3.rs-9883274/v1

License: This work is licensed under a Creative Commons Attribution 4.0 International License.
Read Full License

Additional Declarations: No competing interests reported.

Abstract

Purpose

To evaluate the efficacy of computer-aided navigation (CAN) in improving mandibular contour symmetry during bimaxillary orthognathic surgery with concurrent mandibular contouring, and to compare its accuracy and aesthetic outcomes with conventional double-splint techniques.

Methods

A retrospective cohort study was conducted in 60 patients (30 per group) who underwent bimaxillary orthognathic surgery combined with mandibular contouring. Group A received navigated surgery using the AccuNav-A system for real-time guidance of maxillomandibular complex repositioning and mandibular osteoplasty. Group B underwent conventional surgery with double splints, where mandibular contouring was performed based on the surgeon's experience. The primary outcome was the three-dimensional (3D) discrepancy of reference points at the inferior border of the mandible (RPIBM) between the actual postoperative result and the preoperative virtual plan. Secondary outcomes included facial aesthetic scores assessed by blinded clinicians on a 0–10 scale.

Results

The mean 3D discrepancy was significantly smaller in Group A than in Group B (1.91 mm vs. 4.03 mm, $P < 0.001$). Group A also showed significantly smaller deviations from the mid-sagittal, Frankfort horizontal, and coronal planes. Postoperative facial aesthetic scores were significantly higher in Group A (9.55 ± 0.81) than in Group B (7.82 ± 0.68, $P = 0.01$), with comparable baseline scores ($P = 0.12$). No major complications were observed in either group.

Conclusion

Computer-aided navigation significantly improves the accuracy of mandibular contouring osteoplasty and achieves better postoperative mandibular symmetry and facial aesthetics than conventional double-splint techniques. CAN is a valuable adjunct for orthognathic surgery, particularly in patients requiring precise symmetrical bone reduction.

Clinical trial registration

This study is a retrospective analysis of routine clinical data. All patients received standard surgical care according to institutional protocols; no intervention was prospectively assigned for research purposes.

Therefore, this study does not meet the definition of a clinical trial under ICMJE or WHO ICTRP guidelines, and clinical trial registration is not applicable.

Introduction

Orthognathic surgery is widely regarded as the most definitive and effective surgical intervention for correcting malocclusion resulting from skeletal disharmony in the dentofacial region. The rapid advancement of three-dimensional (3D) imaging, computer-assisted virtual surgical planning (VSP), and computer-aided design and manufacturing (CAD/CAM) technologies has significantly improved the reliability of surgical planning, the precision of operative execution, and the predictability of postoperative outcomes [1–4]. However, because of the mobility of the mandible and temporomandibular joint, particularly in patients with unstable condyle-fossa relations and repeated intraoperative measurement for maxillary repositioning [5–7], the accurate transfer of the preoperative orthognathic surgical plan using CAD/CAM occlusal splints during surgery remains challenging [8].

In addition, because of inherent asymmetries in the height and width of the bilateral mandibular bodies, mandibular asymmetry may persist following the rigid internal fixation of the maxilla and mandible [9]. At this stage, further mandibular contouring is often required, which may involve mandibular angle resection or osteoplasty of the inferior border of the mandible [10]. Accurately contouring the mandible to achieve optimal symmetry based solely on empirical judgment remains a significant challenge.

In the surgical specialties of maxillofacial trauma, oncology, and orthognathic surgery, computer-aided navigation (CAN) serves as a critical tool for augmenting procedural precision and operative safety. This enhancement is achieved through three primary mechanisms: the accurate spatial positioning of bone grafts or synthetic implants, the execution of targeted tumor resections with improved margins, and the deliberate intraoperative avoidance of vital anatomical structures, such as neurovascular bundles and articular compartments [11, 12]. In orthognathic surgery, the integration of computer-assisted navigation has been demonstrated to enable precise intraoperative transfer of preoperative surgical plans. Following the importation of the virtual surgical design into the navigation workstation, the maxilla and mandible can be repositioned and secured according to the real-time spatial guidance provided by a navigation probe, thereby achieving accurate implementation of the planned skeletal movements [13–15]. However, the application of computer-aided navigation for guiding mandibular contouring osteoplasty has been scarcely documented in the literature.

This study aimed to evaluate the efficacy of computer-aided navigation in mandibular contouring surgery by quantitatively comparing postoperative mandibular symmetry between a conventional surgical cohort and a cohort utilizing intraoperative navigation following orthognathic procedures.

Materials and Methods

Patients

This retrospective cohort study was approved by the Ethics Committee of the Affiliated Hospital of Qingdao University (No. QDFYWZLL30553) and followed the Declaration of Helsinki. Because of the retrospective nature of the analysis, the requirement for additional written informed consent for research purposes was waived by the ethics committee; however, all patients had provided written informed consent for their surgical procedures as part of routine clinical care.

We retrospectively reviewed consecutive adult patients who underwent bimaxillary orthognathic surgery combined with mandibular contouring at our department between January 2024 and January 2025.

The inclusion criteria were as follows:

1. Adult patients with congenital dentomaxillofacial deformities planned for bimaxillary orthognathic surgery, with concurrent mandibular contouring planned as part of the same operative procedure.
2. Surgery to be performed using either computer-aided navigation (CAN) or conventional double-splint guidance.

Patients meeting any of the following criteria were excluded:

1. Diagnosis of cleft lip and/or palate.

2. Skeletal deformity secondary to trauma or tumor resection.

3. Planned single-jaw surgery.

4. Requirement for segmental maxillary osteotomy.

The sample size for this study was determined a priori based on the results of a pilot experiment. In the pilot study (n=5 per group), the mean difference from the standard regimen was 2.21 mm (SD=1.15) in the experimental group and 3.78 mm (SD=1.66) in the standard treatment group. These values yielded a pooled standard deviation of 1.428 and a Cohen's d effect size of 1.10. Given the risk of effect size inflation inherent in small pilot samples, a conservative effect size (d=0.8) was adopted for the formal sample size calculation. A two-sided type I error rate (α) of 0.05 and a statistical power (1−β) of 0.80 were specified. Using the standard formula for two independent samples of equal size, the minimum required number of participants was calculated to be 25 per group. To account for an anticipated dropout rate of 20%, the final enrollment was set at 30 participants per group, resulting in a total sample size of 60.

A total of 60 patients (22 males, 38 females; mean age 23.6 years, range 18–38 years) were included. Patients were allocated to two groups based on the surgical technique they actually received, without randomization: Group A (n=30) received navigation-assisted surgery using the AccuNav-A system; Group B (n=30) underwent conventional surgery with double splints. Group assignment was determined by the availability of the navigation system and the operative team's preference during the study period. All surgical procedures were performed by the same operative team.

Computer Assisted Virtual Surgery

Computed tomography (CT) scans (Discovery CT750HD, GE Healthcare, Milwaukee, WI, USA) were obtained preoperatively and at 6-8 months postoperatively. The preoperative CT data were imported into a computer workstation to reconstruct a three-dimensional (3D) model of the skull. Virtual orthognathic surgery was then conducted using Mimics software (version 20.0; Materialise, Leuven, Belgium). The surgical simulation involved planning the direction and magnitude of maxillary movement based on the cephalometric data. The position of the maxillomandibular complex (MMC) was iteratively adjusted until a satisfactory outcome was achieved from multiple viewing angles, considering key parameters such as the anteroposterior position of the MMC, occlusal plane orientation, and overall facial symmetry. Following this, procedures for symmetrizing the bilateral inferior border of the mandible and mandibular osteoplasty were simulated to achieve a symmetrical mandibular contour. The finalized surgical simulation data from Mimics were exported to a surgical navigation workstation. In accordance with the standard protocol for bimaxillary orthognathic surgery, patient-specific maxillary osteotomy guide plates and occlusal splints were designed based on the virtual plan and fabricated using a 3D printer (Perfactory P4K, Huarong Printing, China).

Operation Aided with CAN/Splints

For Group A, after the induction of general anesthesia, a navigation reference frame was installed on the patient's calvarium. The preoperative CT data and the final surgical protocol (STL file) were imported into the AccuNav-A surgical navigation workstation (UEG Medical, Shanghai, China). Registration and accuracy verification were then performed. The 3D model of the surgical design protocol was hidden, and only the preoperative 3D model was exposed. When the navigation probe was pointed at a certain point in the oral cavity, the tip of the navigation stick was displayed on the screen of the navigation workstation.

During the operation, under the guidance of the navigation stick, the maxillomandibular complex was positioned to the preoperatively designed position, and rigid internal fixation (RIF) was performed with titanium plates and screws at the piriform rim, zygomatic buttress, and external oblique line of the mandible. To achieve the final surgical plan, osteoplasty of the inferior border of the mandible was performed under the guidance of the navigation stick, including mandibular angle curved ostectomy (MACO) and outer cortex grinding (OCG) techniques. A ball-tipped surgical burr was subsequently employed to remove the predetermined excess bone, ensuring congruence with the preoperative virtual surgical plan. Throughout the osteotomy procedure, the depth of bone resection was continuously monitored in real time using the navigation probe. For this purpose, a personalized navigation stick (PNS) was assembled using a 20 mL disposable syringe. Because the tip of the PNS could penetrate the skin and touch the cortical bone surface of the lower margin of the mandible, the mandibular contour could be ground more accurately under the guidance of the PNS, including in specific areas such as the mandibular angle, where restricted access limited the use of a conventional navigation probe.

For Group B, under the guidance of a prefabricated osteotomy template, Le Fort I osteotomy was performed on the maxilla. The maxilla was repositioned and stabilized using an intermediate occlusal splint. Following this, RIF of the maxilla was performed. Subsequently, bilateral sagittal split ramus osteotomies (SSRO) of the mandible were performed. The position of the mandibular proximal (condylar) segments was established and maintained using a final occlusal splint. RIF was then accomplished via the placement of osteosynthesis plates along the external oblique lines on both sides of the mandible. Finally, the primary surgeon proceeded with the planned mandibular contouring surgery. The surgical maneuvers were executed based on the preoperative virtual surgical plan, supplemented by the surgeon's experience and intraoperative visual assessment, with the goal of achieving optimal bilateral mandibular symmetry.

Blinding

The operating surgeons could not be blinded to the allocated intervention because of the inherent differences between the surgical techniques. However, all outcome assessors were blinded to group assignment. Specifically, the three clinicians who performed the facial aesthetic evaluations were unaware of whether the photographs were from Group A or Group B, and the order of preoperative and postoperative images was randomized. The radiologist who measured the three-dimensional discrepancies was also blinded to the group allocation. Patients were not formally blinded to the type of surgery they received, but they did not participate in any outcome assessment that could introduce bias.

Evaluation Methods

In this study, the preoperative virtual surgical plan was used as the gold standard, and the actual surgical outcomes were compared with virtual surgical plan. The linear distance discrepancy between the postoperative and preoperative mandibular border reference points was evaluated. A smaller discrepancy relative to the preoperative plan indicated better postoperative symmetry of the mandibular contour. In addition, a blinded clinical assessment of patients' facial aesthetics was performed by clinicians both preoperatively and postoperatively to provide a supplementary subjective evaluation of surgical efficacy.

Quantitative Analysis of Postoperative Results

Both the preoperative virtual surgical plan and the postoperative CT data were imported into medical image processing software (Mimics, Materialise NV). Following voxel-based registration and superimposition, with the anterior cranial base as the stable reference structure, 3D craniofacial skeleton models were generated for both the planned and the actual postoperative conditions. Three anatomical reference planes were subsequently established to define the spatial coordinate system: the Frankfort Horizontal (FH) plane, the mid-sagittal plane (MSP) (constructed perpendicular to the FH plane and

containing the nasion and basion landmarks), and a coronal reference plane (defined as perpendicular to the FH plane and passing through the sella) (Table 1).

Upon establishing the 3D coordinate system, including the primary reference plane and its associated orthogonal planes (Table1), reference points at the inferior border of the mandible (RPIBM) were identified in both the preoperative plan and the postoperative 3D model. For each corresponding point, the linear distance to the primary 3D reference plane was measured. Subsequently, the software automatically computed the absolute discrepancy in these distances for each pair of planned versus achieved reference point positions.

For all cases in Group A and Group B, the three-dimensional positional discrepancies between corresponding RPIBM in the preoperative plan and the postoperative outcome model were calculated and analyzed separately for each group.

Facial Aesthetic Assessment

Preoperative and postoperative standardized facial photographs (frontal, lateral, and 45-degree oblique views) were obtained for all patients in Group A and Group B. Three independent senior clinicians (orthognathic surgeons and orthodontists, each holding the title of Associate Chief Physician), who were not involved in the surgical procedures and were completely blinded to group allocation and the time point (preoperative vs. postoperative), rated each photograph using a simple 0–10 numerical scale (0=worst, 10=best), with a higher score indicating a superior aesthetic outcome [16]. The photographs were randomized and anonymized before presentation; no patient-identifying information or surgical details were disclosed. The final score for each patient and time point was calculated as the mean of the three evaluators' ratings. This scale was chosen for its clinical feasibility and because no validated Chinese-language facial aesthetic instrument was available for this specific patient population at the time of study design. The intraclass correlation coefficient (ICC, two-way random, absolute agreement) was calculated to assess inter-rater reliability.

Statistical analysis

The measurement and data analysis was performed by two uniformly trained maxillofacial surgeons. Each observer measured each distance three times to ensure intraobserver reliability, and the mean observation of the two surgeons was taken as the result. Reliability was calculated using Pearson's intraclass correlation coefficient (ICC, two-way random, absolute agreement). The automated measurement function of Mimics software ensures consistent and objective quantification of spatial deviations. The mean of the two observers' measurements was used as the final value for each parameter.

Facial aesthetic scores were compared between the preoperative and postoperative periods. Quantitative data are presented as the mean±standard deviation. Intergroup differences were analyzed using the independent samples *t*-test. Intragroup differences were assessed using the paired samples *t*-

test. Analysis was performed using SPSS 22.0 (IBM Corp., Armonk, NY, USA). Statistical significance was specified at $P < 0.05$.

This retrospective cohort study is reported in accordance with the STROBE guidelines for observational studies.

Clinical trial registration

This study is a retrospective analysis of routine clinical data. All patients received standard surgical care according to institutional protocols; no intervention was prospectively assigned for research purposes. Therefore, this study does not meet the definition of a clinical trial under ICMJE or WHO ICTRP guidelines, and clinical trial registration is not applicable.

Results

For the discrepancy analysis of the RPIBM, both intra-observer (ICC = 0.88, 95% CI: 0.81–0.92) and inter-observer (ICC = 0.89, 95% CI: 0.83–0.94) reliabilities were high. For the facial aesthetic assessment, the inter-rater agreement was also excellent, with an ICC of 0.85 (95% CI: 0.78–0.90) for preoperative scores and 0.87 (95% CI: 0.81–0.92) for postoperative scores.

In this comparative analysis, the two groups demonstrated distinct patterns in the positional deviation of the RPIBM relative to the primary 3D reference plane between the actual surgical outcomes and the preoperative virtual surgical plan. The mean deviation of point Pg from the mid-sagittal plane (MSP) was 1.46 mm in Group A and 3.48 mm in Group B. In terms of maximum deviation from the MSP, the point Go exhibited the largest divergence in both groups, with values of 2.43 mm in Group A and 5.24 mm in Group B. Regarding the Frankfort horizontal (FH) plane, the greatest deviation in Group A was observed at point No (2.82 mm), whereas in Group B, the maximum deviation from the FH plane occurred at point L6 (7.35 mm). For the coronal plane (CP), point Go showed the largest deviation in Group A (2.46 mm), while in Group B, the maximum CP deviation was recorded at point L7 (4.85 mm). (Table 1)

Analysis of the bilateral RPIBM revealed substantial inter-group differences in their positional relationships to the primary anatomical reference planes. The mean absolute distance from the bilateral points to the mid-sagittal plane (MSP) was 1.77 mm in Group A and 3.35 mm in Group B, indicating markedly greater bilateral asymmetry relative to the midline in Group B. For the Frankfort horizontal (FH) plane, the mean absolute distance was 2.02 mm in Group A and 5.14 mm in Group B. Similarly, for the coronal plane (CP), the corresponding values were 1.92 mm in Group A and 3.58 mm in Group B. Overall, the differences between the two groups in surgical accuracy were statistically significant. The mean three-dimensional (3D) discrepancy of the RPIBM was 1.91 mm for Group A, compared with 4.03 mm for Group B. (Table 1)

The mean differences (Group B – Group A) for all indices were positive and ranged from 0.46 mm (MSP-L2) to 5.19 mm (FHP-L6), with 95% confidence intervals that did not include zero in the vast majority of cases (see Table 1, column “Mean difference [95% CI]”). For example, at point Pg relative to

the FHP plane, the mean difference was 1.36 mm (95% CI: 0.79 to 1.93 mm; P = 0.01). The only exceptions with confidence intervals approaching or crossing zero were MSP-Fo (0.68 mm [0.08, 1.28]) and CP-L2 (0.57 mm [0.16, 0.98]), although both remained statistically significant ($P \leq 0.02$). Overall, Group B consistently showed larger discrepancies from the virtual plan than Group A, indicating poorer postoperative accuracy relative to the preoperative design.

Table 2 summarizes the changes in facial aesthetic scores before and after surgery in both groups. In Group A, the mean aesthetic score improved significantly from 3.18 preoperatively to 9.55 postoperatively ($P < 0.001$). Similarly, Group B showed a significant increase from 2.95 to 7.82 ($P < 0.001$). Preoperatively, there was no statistically significant difference between the two groups ($P = 0.12$). However, postoperatively, Group A achieved a significantly higher aesthetic score than Group B (9.55 ± 0.81 vs. 7.82 ± 0.68; $P = 0.01$). These findings indicate that both surgical techniques produced substantial aesthetic improvements, with Group A demonstrating superior postoperative facial aesthetics compared with Group B. (Table 2)

Perioperative Outcomes and Complications

Intraoperative and postoperative complications, adverse events, and relevant perioperative parameters are summarized in Table 3. In Group A, the mean operative time was 235.5 min, and the mean estimated blood loss was 285.4 mL. In Group B, the mean operative time was 218.3 min, and the mean estimated blood loss was 272.5 mL. No statistically significant differences were observed between the two groups for either parameter ($P = 0.38$ and $P = 0.42$, respectively).

Regarding navigation-specific issues in Group A, registration was successfully completed in all 30 cases. In two patients (6.7%), the initial registration accuracy was suboptimal (target registration error > 1.5 mm) and required a second registration attempt, which was successful. No complete navigation system failure or equipment malfunction occurred. The mean registration time (from reference frame placement to accuracy verification) was 16.2 min.

With respect to nerve injury, no patient in either group developed persistent inferior alveolar nerve or facial nerve dysfunction. One patient in Group B (3.3%) experienced transient hypoesthesia of the mental nerve on the operated side, which resolved completely within six weeks postoperatively. No hardware-related complications (e.g., plate fracture, screw loosening, or malposition) or surgical site infections were observed in either group. No patient required revision surgery for asymmetry or any other cause during the follow-up period. No intraoperative adverse events (e.g., unexpected bleeding, unfavorable fracture, or damage to adjacent structures) were recorded in either group.

Discussion

This study quantitatively evaluated postoperative mandibular contour symmetry following simultaneous mandibular contouring during bimaxillary orthognathic surgery, comparing navigated and conventional techniques. The findings revealed significantly superior mandibular symmetry in the navigation-aided

group. These results confirm both the technical feasibility and the enhanced procedural accuracy of intraoperative navigation for simultaneous mandibular contouring in bimaxillary orthognathic surgery.

Residual asymmetry following orthognathic surgery remains a common clinical challenge, often necessitating adjunctive mandibular osteoplasty. Chen et al [17] observed that noticeable chin deviation persists postoperatively, a condition influenced by residual asymmetry of the mandibular body, chin, and ramus. Similarly, Ajmera et al [18] demonstrated that although bimaxillary surgery achieves significant correction, asymmetry can persist at multiple anatomical sites, frequently requiring subsequent secondary procedures.

The simultaneous performance of orthognathic surgery and facial bone contouring has been reported in the literature. These studies have demonstrated the feasibility of combining procedures such as orthognathic surgery with mandibular angle ostectomy (MAO), mandibular border ostectomy (MBO), mandibular outer cortex grinding (MOCG), and zygomatic body and arch reduction [19–22]. However, achieving precise and symmetrical contouring through conventional surgical guides remains challenging. The resulting contour is often irregular and uneven, with difficulties in ensuring bilateral symmetry. Critical intraoperative considerations include preventing either excessive or insufficient bone resection and accurately controlling the extent and progression of the osteotomy [23].

Transfer of the surgical plan to the operating room was usually accomplished using conventional double-splint technology (intermediate and final splint), including the CAD/CAM splints [15, 24–29]. In mandibular contouring procedures, the most widely adopted auxiliary technique involves the use of osteotomy or bone-shaping guides. These guides are typically utilized intraoperatively to demarcate the precise region for bone resection or grinding. Following this delineation, a reciprocating saw or round burr is employed to execute the planned osteotomy or grinding process [30, 31]. However, their application presents challenges in partial or small-scale bone reduction procedures, where the intended resection is often on the order of a few millimeters. In such cases, guide placement can be technically difficult, particularly within confined surgical spaces requiring protection of the mental nerve and avoidance of iatrogenic angular injury due to excessive tissue traction. Liu et al. [32] reported that while designing a perforated osteotomy line improved operational accuracy, the incidence of complications—including nerve injury, excessive bone resection, and bilateral asymmetry—remained as high as 9.2%. Furthermore, as noted by Ellis et al. [33], surgical splints primarily guide osteotomy precision in the transverse and sagittal dimensions; achieving vertical precision still relies heavily on the surgeon's intraoperative judgment and manual measurement.

The application of computer-aided navigation (CAN) in the correction of maxillofacial deformities has been increasingly reported [2, 10, 34–41]. The real-time tracking and three-dimensional visualization of mobilized bone segments provide surgeons with vivid and dynamic feedback during the repositioning procedure. This technological integration enables the continuous display of the spatial relationship between the planned and actual positions of bone segments on-screen, thereby facilitating precise intraoperative guidance and enhancing surgical accuracy [35, 42, 43]. Consequently, surgical outcomes

can be verified intraoperatively, enabling immediate adjustments to ensure precise execution of the preoperative plan and achieve satisfactory results [42, 44]. For instance, Mazzoni et al. [39] utilized 3-Matic software to superimpose pre- and postoperative datasets and highlighted the advantage of navigation in improving vertical control of the maxilla compared to conventional splints. Similarly, Badialdi et al. [45] employed both surface-to-surface and point-based analyses, confirming superior accuracy, particularly in the vertical dimension. Shirota et al. [43] reported that the position of the maxillary segment repositioned using a CAD/CAM splint was highly consistent with the virtual plan when verified with a navigation system, thereby confirming its clinical accuracy. Despite these advancements in maxillary positioning, quantitative evaluations of the contouring outcomes achieved in mandibular osteoplasty - whether using conventional osteotomy guides or CAN - remain scarcely reported in the literature.

According to published literature, the precision of the virtual surgical plan is effectively transferred intraoperatively, with the majority of results within margins of clinical significance (< 2 mm) [1, 13, 46, 47]. With real-time navigation guidance, more accurate and reliable repositioning of the down-fractured maxilla can be achieved during orthognathic surgery [44, 48]. The present study compared the accuracy of transferring the preoperative virtual surgical plan to the actual postoperative position between two surgical techniques. Group A consistently exhibited smaller mean deviations from all three reference planes (MSP, FHP, and CP) compared with Group B. Notably, within-Group A analyses showed no statistically significant deviations at any measured point (all $P > 0.05$), indicating that the surgical outcomes faithfully reproduced the virtual plan. In contrast, Group B demonstrated significant deviations at virtually all points ($P < 0.05$ for most indices), with particularly large discrepancies at points L6 (7.35 mm) and L3 (6.38 mm) relative to the Frankfort horizontal plane. The overall three-dimensional discrepancy was 1.91 mm in Group A versus 4.03 mm in Group B. These findings suggest that the technique used in Group A enables significantly higher precision and better positional control in mandibular osteoplasty.

Between-group comparisons further confirmed the advantage of Group A. All mean differences (Group B minus Group A) were positive, with 9 % confidence intervals excluding zero for the vast majority of indices (e.g., FHP-L6: 5.19 mm [5 % CI: 3.82–6.56 mm]; $P < 0.001$). The mean absolute distances of bilateral points to the reference planes were consistently lower in Group A (MSP: 1.77 mm vs. 3.35 mm; FH: 2.02 mm vs. 5.14 mm; CP: 1.92 mm vs. 3.58 mm), reflecting superior bilateral symmetry. These objective measurements align with the aesthetic outcomes presented in Table 2, where Group A achieved significantly higher postoperative facial aesthetic scores (9.55 vs. 7.82 ; $P = 0.01$). Therefore, the enhanced surgical precision observed in Group A directly translated into better clinical and aesthetic results. While the assessment of positional discrepancies is subject to inherent registration errors of cone-beam computed tomography (CBCT), and the clinical relevance of sub-millimeter differences requires further validation, our findings support the preferential use of the Group A technique–specifically, computer-aided navigation (CAN)–when precise replication of the virtual surgical plan is critical for achieving optimal symmetry and facial aesthetics. This is consistent with our previous findings [44].

A comparative analysis of aesthetic scores for facial contours was performed between preoperative and postoperative cohorts. The assessment revealed that both surgical techniques led to significant improvements in facial aesthetic scores, confirming their clinical efficacy in mandibular contouring or orthognathic procedures. Notably, although the two groups had comparable baseline scores (P = 0.12), Group A achieved a significantly higher postoperative score than Group B (9.55 ± 0.81 vs. 7.82 ± 0.68; P = 0.01), indicating that the technique used in Group A confers superior aesthetic outcomes. This advantage may be attributed to the greater surgical precision observed in Group A, as reflected by the smaller discrepancies from the virtual surgical plan across all reference planes (Table 1), which likely translates into better facial symmetry and contour harmony. The larger magnitude of improvement in Group A (Δ = 6.37) compared with Group B (Δ = 4.87) further supported this interpretation. Nevertheless, several limitations should be acknowledged. Aesthetic assessment, despite being performed by blinded clinicians, remains inherently subjective, and the use of a single-scale score may not capture all dimensions of facial aesthetics, such as profile balance or soft-tissue texture. Future studies should incorporate patient-reported outcome measures (PROMs) and three-dimensional photogrammetric analysis to provide a more comprehensive evaluation. The Group A protocol appears to yield superior postoperative aesthetics and may be preferred when optimizing facial outcomes is a primary surgical goal.

However, it is noteworthy that the absolute distances from the RPIBM to the reference planes were consistently larger than those measured from maxillary and dental reference points. This observation can be attributed to the biomechanical principle by which the skull base serves as the center of rotation during maxillomandibular complex repositioning. As the maxilla is anatomically closer to this rotational center, its planned movement results in a proportionally greater displacement—or amplification effect—at the more distant mandibular inferior border. This phenomenon explains the observed larger positional variance at the mandibular contour for a given surgical movement, a finding that aligns with established biomechanical principles reported in prior studies [33, 44, 49].

An additional advantage of CAN is its capacity for immediate intraoperative error detection and real-time correction[2, 34, 41]. The final position of the mandible is biomechanically dependent on the position of the maxilla. A minor deviation in maxillary repositioning is geometrically amplified when projected onto the mandible, particularly affecting the proximal segments, thereby resulting in a disproportionately larger mandibular discrepancy [50]. Crucially, even if a slight maxillary positional deviation occurs intraoperatively—provided a stable occlusal relationship is achieved—resulting mild mandibular asymmetry can be effectively compensated for through subsequent mandibular contouring. While a subtle tilt of the occlusal plane may be clinically inconspicuous, asymmetry of the bilateral mandibular border has a pronounced impact on facial aesthetics. Therefore, by symmetrically recontouring the mandibular border during the osteoplasty procedure, the overall facial symmetry can be restored, effectively remedying deviations originating from an imperfectly positioned maxillomandibular complex.

The confined intraoral operating space presented a significant challenge for accessing the middle and posterior regions of the mandibular border with a standard navigation probe. While an intraoral incision

is preferred to avoid visible postoperative scars, the resulting surgical exposure is inherently narrow and limited, offering a suboptimal operative field [51]. To address this limitation, we utilized a specially adapted navigation probe with a sharp, fine needle tip. This design allowed the tip to percutaneously access the mandibular cortical bone surface without requiring an extensive skin incision, thereby eliminating the risk of a visible scar. Consequently, this modified instrument enabled accurate navigation and contouring in anatomical areas that are otherwise inaccessible to conventional navigation probes.

Limitations

This study is subject to several limitations. First, the sample size was modest and all participants were recruited from a single institution, potentially limiting the generalizability of the findings. Second, the surgeon-assembled personalized navigation probe, although practical, lacked a standardized protocol for fabrication, calibration, and accuracy verification. Third, blinding of surgeons was infeasible owing to the nature of the procedures, a well-recognized challenge in surgical trials. Fourth, the Frankfort horizontal plane, constructed from bilateral orbital and auricular landmarks, is inherently subjective in patients with facial asymmetry; therefore, results relative to this plane should be interpreted with caution. Future studies should consider using natural head position to improve the reliability of three-dimensional discrepancy analyses. Fifth, the facial aesthetic assessment used a non-validated 0–10 numerical scale. Although the scale demonstrated excellent inter-rater reliability (ICC > 0.85) and is simple for clinical use, the subjective nature of aesthetic evaluation remains a potential source of bias. Future investigations should incorporate validated instruments (e.g., FACE-Q, POSAS) or objective three-dimensional photogrammetric analysis to complement clinician-based evaluations. Importantly, although patients were not blinded to the intervention, they played no role in outcome assessment, and the outcome assessors (including the three clinicians for aesthetic scores and the radiologist for discrepancy measurements) were fully blinded to group allocation. Therefore, detection bias was minimized despite the lack of patient and surgeon blinding. Larger, multi-centre studies with extended follow-up and standardized navigation protocols are needed to confirm these preliminary findings.

Conclusion

This study demonstrates that computer-aided navigation (CAN)-guided simultaneous mandibular contouring during bimaxillary orthognathic surgery significantly enhances the precision of mandibular osteoplasty, yielding superior postoperative mandibular symmetry and aesthetic outcomes compared with conventional, experience-based techniques. CAN is therefore recommended as a valuable adjunctive tool for mandibular contouring procedures, particularly in complex cases involving unilateral deformity or significant mandibular volumetric asymmetry.

Abbreviations

CAN	Computer-Aided Navigation
3D	Three-Dimensional
RPIBM	Reference Points at the Inferior Border of Mandible
VSP	Virtual Surgical Planning
CAD/CAM	Computer-Aided Design and Manufacturing
CT	Computed Tomography
MMC	Maxillomandibular Complex
STL	Standard Tessellation Language Files
RIF	Rigid Internal Fixation
MACO	Mandibular Angle Curved Ostectomy
OCG	Outer Cortex Grinding
PNS	Personalized Navigation Stick
SSRO	Sagittal Split Ramus Osteotomies
FHP	Frankfort Horizontal Plane
MSP	Mid-Sagittal Plane
CP	Coronal Plane
ICC	Intraclass Correlation Coefficient
MAO	Mandibular Angle Ostectomy
MBO	mandibular border ostectomy
MOCG	mandibular outer cortex grinding
CBCT	cone-beam computed tomography
PROMs	patient-reported outcome measures

Declarations

Acknowledgements

The authors confirm that the funders played no role in the conception, design, data collection, analysis, interpretation, or preparation of the manuscript.

Authors' contributions

All authors contributed to the conception and design of the study. Ningning Sun: writing of the original draft, data collection, data curation, data analysis, and software. Zexian Xu, Yupeng Wu, and Ming Sun: data collection, data measurement, aesthetic scoring, and software. Jian Sun and Yanshan Liu: surgical procedures, guide production, and validation. Qian Yang and Yang Liu: orthodontic treatment and aesthetic scoring. Chen Chen: surgical procedures, writing – review and editing, supervision, data curation, project administration, and resources. All authors read and approved the final manuscript.

Funding

None

Data availability

All data supporting the findings of this study, are stored by the corresponding author. These data are available from the corresponding author upon reasonable request.

Ethics approval and consent to participate

All procedures performed in studies involving human participants were in accordance with the ethical standards of the Ethics Committee of the Affiliated Hospital of Qingdao University (Approval No. QDFYWZLL30553) and with the 1964 Helsinki Declaration and its later amendments or comparable ethical standards. Written informed consent was obtained and signed by all participants prior to their enrollment in the study.

Consent for publication

Not applicable.

Competing interests

The authors declare no competing interests.

Author details

[1] Department of Emergency Intensive Care Unit, The Affiliated Hospital of Qingdao University, No. 16 Jiangsu Road, Qingdao, Shandong 266000, China
[2] Department of Oral and Maxillofacial Surgery, The Affiliated Hospital of Qingdao University, No. 16 Jiangsu Road, Qingdao, Shandong 266000, China
[3] Department of Dental Implantology, The Affiliated Hospital of Qingdao University, No. 16 Jiangsu Road, Qingdao, Shandong 266000, China
[4] Department of Orthodontics, The Affiliated Hospital of Qingdao University, No. 16 Jiangsu Road, Qingdao, Shandong 266000, China

References

1. Hsu SS, Gateno J, Bell RB, Hirsch DL, Markiewicz MR, Teichgraeber JF, Zhou X, Xia JJ. Accuracy of a computer-aided surgical simulation protocol for orthognathic surgery: a prospective multicenter study. J Oral Maxillofac Surg. 2013;71:128-142.
2. Zinser MJ, Mischkowski RA, Dreiseidler T, Thamm OC, Rothamel D, Zoller JE. Computer-assisted orthognathic surgery: waferless maxillary positioning, versatility, and accuracy of an image-guided visualisation display. Br J Oral Maxillofac Surg. 2013;51:827-833.
3. Alkhayer A, Piffko J, Lippold C, Segtto E. Accuracy of virtual planning in orthognathic surgery: a systematic review. Head Face Med. 2020;16:34.
4. Hatamleh MM, Bhamrah G, Ryba F, Mack G, Huppa C. Simultaneous Computer-Aided Design/Computer-Aided Manufacture Bimaxillary Orthognathic Surgery and Mandibular Reconstruction Using Selective-Laser Sintered Titanium Implant. J Craniofac Surg. 2016; 27:1810-4.
5. Omura S, Kimizuka S, Iwai T, Tohnai I. An accurate maxillary superior repositioning technique without intraoperative measurement in bimaxillary orthognathic surgery. Int J Oral Maxillofac Surg. 2012;41:949-51.
6. Yamashita Y, Imai H, Takasu H, Fujita K, Iwai T, Hirota M, Mitsudo K. A Novel Orthognathic Surgery With a Half-Millimeter Accuracy for the Maxillary Positioning Using Prebent Plates and Computer-Aided Design and Manufacturing Osteotomy Guide. J Craniofac Surg. 2023;34:2087-91.
7. Li B, Zhang L, Sun H, Yuan J, Shen SG, Wang X. A novel method of computer aided orthognathic surgery using individual CAD/CAM templates: a combination of osteotomy and repositioning guides. Br J Oral Maxillofac Surg. 2013;51:e239-44.
8. Hoang D, Perrault D, Stevanovic M, Ghiassi A. Surgical applications of three-dimensional printing: a review of the current literature & how to get started. Ann Transl Med. 2016;4:456.
9. Severt TR, Proffit WR. The prevalence of facial asymmetry in the dentofacial deformities population at the University of North Carolina. Int J Adult Orthodon Orthognath Surg. 1997;12:171-6.
10. Bell RB. Computer planning and intraoperative navigation in orthognathic surgery. J Oral Maxillofac Surg. 2011;69:592-605.
11. Baumann A, Schicho K, Klug C, Wagner A, Ewers R. Computer-assisted navigational surgery in oral and maxillofacial surgery. Atlas Oral Maxillofac Surg Clin North Am. 2005;13:41-9.
12. Ewers R, Schicho K, Undt G, Wanschitz F, Truppe M, Seemann R, Wagner A. Basic research and 12 years of clinical experience in computer-assisted navigation technology: a review. Int J Oral Maxillofac Surg. 2005;34:1-8.
13. Stokbro K, Aagaard E, Torkov P, Bell RB, Thygesen T. Virtual planning in orthognathic surgery. Int J Oral Maxillofac Surg. 2014;43:957-65.
14. De Riu G, Virdis PI, Meloni SM, Lumbau A, Vaira LA. Accuracy of computer-assisted orthognathic surgery. J Craniomaxillofac Surg. 2018;46:293-8.
15. Zhang N, Liu S, Hu Z, Hu J, Zhu S, Li Y. Accuracy of virtual surgical planning in two-jaw orthognathic surgery: comparison of planned and actual results. Oral Surg Oral Med Oral Pathol Oral Radiol. 2016;122:143-51.

16. Rustemeyer J, Eke Z, Bremerich A. Perception of improvement after orthognathic surgery: the important variables affecting patient satisfaction. Oral Maxillofac Surg. 2010;14(3):155-62.
17. Chen YF, Liao YF, Chen YA, Chen YR. Surgical-orthodontic treatment for class II asymmetry: outcome and influening factors. Sci Rep. 2019;9:17956.
18. Ajmera DH, Hsung RT, Singh P, Wong NSM, Yeung AWK, Lam WYH, et al. Three-dimensional assessment of facial asymmetry in Class III subjects. Part 1: a retrospective study evaluating postsurgical outcomes. Clin Oral Investig. 2022;26:4947-66.
19. Li Y, Hu Z, Ye B, Liu Y, Ren X, Zhu S. Combined Use of Facial Osteoplasty and Orthognathic Surgery for Treatment of Dentofacial Deformities. J Oral Maxillofac Surg. 2016;74:2501-5.
20. Zhang Y, Sun X, Wang L, Chen K, Wang X, Wu G. Simultaneous Orthognathic Surgery and Mandibular Contour Osteoplasty for Treating Mandibular Protrusion With High Gonial Angle. J Craniofac Surg.2020;31:1362-6.
21. Xiao Y, Sun X, Wang L, Zhang Y, Chen K, Wu G. The Application of 3D Printing Technology for Simultaneous Orthognathic Surgery and Mandibular Contour Osteoplasty in the Treatment of Craniofacial Deformities. Aesthetic Plast Surg.2017;41:1413-24.
22. Song G, Zong X, Guo X, Zhao J, Jin X. Single-Stage Mandibular Curved Ostectomy on Affected Side Combined with Bilateral Outer Cortex Grinding for Correction of Facial Asymmetry: Indications and Outcomes. Aesthetic Plast Surg.2019;43:733-41.
23. Baek SM, Kim SS, Bindiger A. The prominent mandibular angle: preoperative management, operative technique, and results in 42 patients. Plast Reconstr Surg.1989;83:272-80.
24. Xia JJ, Gateno J, Teichgraeber JF, Christensen AM, Lasky RE, Lemoine JJ, et al. Accuracy of the computer-aided surgical simulation (CASS) system in the treatment of patients with complex craniomaxillofacial deformity: A pilot study. J Oral Maxillofac Surg. 2007;65:248-54.
25. Xia J J, Gateno J, Teichgraeber J F, Yuan P, Chen KC, Li J, et al. Algorithm for planning a double-jaw orthognathic surgery using a computer-aided surgical simulation (CASS) protocol. Part 1: planning sequence. Int J Oral Maxillofac Surg. 2015;44:1431-40.
26. Zinser MJ, Mischkowski RA, Sailer HF, Zoller J. Computer-assisted orthognathic surgery: feasibility study using multiple CAD/CAM surgical splints. Oral Surg Oral Med Oral Pathol Oral Radiol. 2012;113:673-87.
27. Xia J, Samman N, Yeung RW, Shen SG, Wang D, Ip HH, et al. Three-dimensional virtual reality surgical planning and simulation workbench for orthognathic surgery. Int J Adult Orthodon Orthognath Surg. 2000;15:265-82.
28. Shaheen E, Shujaat S, Saeed T, Jacobs R, Politis C. Three-dimensional planning accuracy and follow-up protocol in orthognathic surgery: a validation study. Int J Oral Maxillofac Surg. 2019;48:71-6.
29. Schouman T, Rouch P, Imholz B, Fasel J, Courvoisier D, Scolozzi P. Accuracy evaluation of CAD/CAM generated splints in orthognathic surgery: a cadaveric study. Head Face Med. 2015;11:24.
30. Ye N, Long H, Zhu S, Yang Y, Lai W, Hu J. The Accuracy of Computer Image-Guided Template for Mandibular Angle Ostectomy. Aesthetic Plast Surg. 2015;39:117-23.

31. Zhang C, Teng L, Chan FC, Xu JJ, Lu JJ, Xie F, et al. Single stage surgery for contouring the prominent mandibular angle with a broad chin deformity: en-bloc Mandibular Angle-Body-Chin Curved Ostectomy (MABCCO) and Outer Cortex Grinding (OCG). J Craniomaxillofac Surg. 2014;42:1225-33.
32. Liu D, Huang J, Shan L, Wang J. Intraoral curved ostectomy for prominent mandibular angle by grinding, contiguous drilling, and chiseling. J Craniofac Surg. 2011;22:2109-13.
33. Ellis ER. Bimaxillary surgery using an intermediate splint to position the maxilla. J Oral Maxillofac Surg. 1999;57:53-6.
34. Yu H, Shen SG, Wang X, Zhang L, Zhang S. The indication and application of computer-assisted navigation in oral and maxillofacial surgery-Shanghai's experience based on 104 cases. J Craniomaxillofac Surg. 2013;41:770-4.
35. Chen X, Li Y, Xu L, Sun Y, Politis C, Jiang X. A real time image-guided reposition system for the loosed bone graft in orthognathic surgery. Comput Assist Surg (Abingdon). 2021;26:1-8.
36. Huang L, Liu Y, Zhu Z, Luo E. Application of mixed reality bone registration and positioning technology in orthognathic surgery. Int J Oral Maxillofac Surg. 2024;54:346-51.
37. Lin HH, Lo LJ. Three-dimensional computer-assisted surgical simulation and intraoperative navigation in orthognathic surgery: a literature review. J Formos Med Assoc. 2015;114:300-7.
38. Tsuji M, Noguchi N, Shigematsu M, Yamashita Y, Ihara K, Shikimori M, et al. A new navigation system based on cephalograms and dental casts for oral and maxillofacial surgery. Int J Oral Maxillofac Surg. 2006;35:828-36.
39. Mazzoni S, Badiali G, Lancellotti L, Babbi L, Bianchi A, Marchetti C. Simulation-guided navigation: a new approach to improve intraoperative three-dimensional reproducibility during orthognathic surgery. J Craniofac Surg. 2010;21:1698-1705.
40. Shim BK, Shin HS, Nam SM, Kim YB. Real-time navigation-assisted orthognathic surgery. J Craniofac Surg. 2013;24:221-5.
41. Sun Y, Luebbers HT, Agbaje JO, Lambrichts I, Politis C. The accuracy of image-guided navigation for maxillary positioning in bimaxillary surgery. J Craniofac Surg. 2014;25:1095-9.
42. Chen C, Sun N, Jiang C, Sun J. Randomized Controlled Clinical Trial to Assess the Utility of Computer-Aided Intraoperative Navigation in Bimaxillary Orthognathic Surgery. J Craniofac Surg. 2021;32:2205-9.
43. Shirota T, Shiogama S, Asama Y, Tanaka M, Kurihara Y, Ogura H, et al. CAD/CAM splint and surgical navigation allows accurate maxillary segment positioning in Le Fort I osteotomy. Heliyon. 2019;5:e2123.
44. Chen C, Sun N, Jiang C, Liu Y, Sun J. Accurate transfer of bimaxillary orthognathic surgical plans using computer-aided intraoperative navigation. Korean J Orthod. 2021;51:321-8.
45. Badiali G, Roncari A, Bianchi A, Taddei F, Marchetti C, Schileo EV. Navigation in Orthognathic Surgery: 3D Accuracy. Facial Plast Surg. 2015;31:463-73.

46. Bouchard C, Landry PE. Precision of maxillary repositioning during orthognathic surgery: a prospective study. Int J Oral Maxillofac Surg. 2013;42:592-6.
47. Donatsky O, Bjorn-Jorgensen J, Holmqvist-Larsen M, Hillerup S. Computerized cephalometric evaluation of orthognathic surgical precision and stability in relation to maxillary superior repositioning combined with mandibular advancement or setback. J Oral Maxillofac Surg. 1997;55:1071-80.
48. Ong TK, Banks RJ, Hildreth AJ. Surgical accuracy in Le Fort I maxillary osteotomies. Br J Oral Maxillofac Surg. 2001;39:96-102.
49. Xia JJ, Shevchenko L, Gateno J, Teichgraeber JF, Taylor TD, Lasky RE, et al. Outcome study of computer-aided surgical simulation in the treatment of patients with craniomaxillofacial deformities. J Oral Maxillofac Surg. 2011;69:2014-24.
50. Hu P, Li J, Du W, Ji H, Xu C, Luo E. The Drilling Guiding Templates and Pre-Bent Titanium Plates Improves the Operation Accuracy of Orthognathic Surgery With Computer-Aided Design and Computer-Aided Manufacturing Occlusal Splints for Patients With Facial Asymmetry. J Craniofac Surg. 2019;30:2144-8.
51. Lei R, Wang Y, Xu S, Hong F, Xu M, Wei L, et al. A modified intraoral and extraoral approach osteotomy for the prominent mandibular angle. J Plast Reconstr Aesthet Surg. 2017;70:1091-100.
52.

Tables

Table 2 Assessment of Facial Aesthetic Changes Before and After Surgery in Two Groups

Group	Preoperative Score	Postoperative	*P*
A (n=30)	3.18±0.64	9.55±0.81	0.001
B (n=30)	2.95±0.57	7.82±0.68	0.001
P	0.12	0.01	

Data are presented as mean ± standard deviation. The aesthetic scores were assessed by three clinicians who were blinded to group allocation and to the time point (preoperative vs. postoperative). The intraclass correlation coefficient (ICC, two-way random, absolute agreement) for the three raters was 0.85 (95% CI: 0.78–0.90) for preoperative scores and 0.87 (95% CI: 0.81–0.92) for postoperative scores, indicating excellent inter-rater reliability. P0.05 was significant.

Table 1 Discrepancy Analysis of RPIBM Relative to the Three-Dimensional Reference Planes: A Comparative Study Between Preoperative Planning (T_0) and Postoperative Outcomes (T_1) in Group A and Group B

Index	Group A (n=30)		Group B (n=30)		Mean difference (B-A) [95% CI]	*P(between)*
	T_1-T_0	*P*	T_1-T_0	*P*		
Distance to FHP(mm)						
Pg	1.62±0.69	0.34	2.98±1.44	0.01	1.36 (0.79, 1.93)	0.01
Fo	2.07±1.49	0.58	3.36±1.83	0.01	1.29 (0.45, 2.13)	0.00
Go	2.13±2.15	0.46	5.62±3.41	0.04	3.49 (2.05, 4.93)	0.00
L2	1.82±1.11	0.31	4.84±3.27	0.03	3.02 (1.78, 4.26)	0.03
L3	1.56±0.99	0.16	6.38±7.48	0.02	4.82 (2.12, 7.52)	0.00
L6	2.16±1.12	0.25	7.35±3.67	0.01	5.19 (3.82, 6.56)	0.00
L7	2.03±1.36	0.45	5.57±3.82	0.00	3.54 (2.09, 4.99)	0.02
No	2.82±1.26	0.18	5.22±4.82	0.00	2.40 (0.62, 4.18)	0.00
Distance to MSP(mm)						
Pg	1.46±0.46	0.29	3.48±1.57	0.00	2.02 (1.43, 2.61)	0.02
Fo	2.13±0.87	0.48	2.81±1.43	0.00	0.68 (0.08, 1.28)	0.00
Go	2.43±1.56	0.39	5.24±1.63	0.03	2.81 (2.00, 3.62)	0.00
L2	0.82±0.53	0.28	1.28±0.86	0.02	0.46 (0.10, 0.82)	0.00
L3	1.26±1.03	0.51	2.83±1.86	0.01	1.57 (0.81, 2.33)	0.00
L6	1.88±1.12	0.47	3.19±1.36	0.00	1.31 (0.68, 1.94)	0.00
L7	1.95±1.60	0.62	4.26±1.28	0.02	2.31 (1.58, 3.04)	0.00
No	2.24±1.17	0.25	3.72±1.54	0.04	1.48 (0.79, 2.17)	0.00
Distance to CP(mm)						
Pg	1.88±0.75	0.12	3.77±1.29	0.00	1.89 (1.36, 2.42)	0.00
Fo	1.91±1.39	0.55	3.58±1.73	0.02	1.67 (0.88, 2.46)	0.02
Go	2.46±1.64	0.37	4.27±1.84	0.02	1.81 (0.93, 2.69)	0.00
L2	1.25±0.78	0.49	1.82±0.85	0.01	0.57 (0.16, 0.98)	0.00

L3	1.23±0.80	0.31	3.86±1.59	0.00	2.63 (1.99, 3.27)	0.00
L6	2.18±1.37	0.26	3.85±2.03	0.03	1.67 (0.79, 2.55)	0.00
L7	2.24±1.55	0.62	4.85±2.27	0.00	2.61 (1.63, 3.59)	0.00
No	2.19±1.84	0.28	3.91±1.36	0.01	1.72 (0.90, 2.54)	0.00

Data are presented as mean (standard deviation). Independent-samples *t*-test was used for between-group comparisons.

Definition of landmarks and parameters

Dental landmarks:

L1: Midpoint of the contact area between the mandibular central incisors.

L2: Midpoint of the incisal edge of the mandibular lateral incisor.

L3: Cusp tip of the mandibular canine.

L6: Mesiobuccal cusp of the mandibular first molar.

L7: Mesiobuccal cusp of the mandibular second molar.

Skeletal landmarks

Pg (Pogonion): Most anterior point of the mental symphysis.

Fo (Mental foramen): Center of the mental foramen.

No (Ramus point): Most anterior point on the mandibular ramus at its intersection with the occlusal plane.

Go (Gonion): Most posterolateral point of the mandibular angle.

Definition of measurement planes and linear measurements

Sagittal plane
A plane parallel to the mid-sagittal plane (MSP) passing through point L2 was defined. Its intersection with the lower border of the mandible was designated as L2-L/R.

Coronal/oblique planes
A plane perpendicular to the Go-Pg plane passing through point L3 was defined. Its intersection with the lower border of the mandible was designated as L3-L/R. The points Fo-L/R, L6-L/R, L7-L/R, and No-L/R were defined analogously.

Linear measurements

Pg: Perpendicular distance from Pg to the coronal plane (CP), Frankfort horizontal (FH) plane, or MSP.

Go: Difference between the perpendicular distances from the bilateral Go points to the CP, FH, and MSP. The definition for Fo (underlined) is analogous.

L2: Mean absolute difference between the postoperative and preoperative distances from the bilateral L2-L/R points to the three-dimensional reference plane. This metric quantifies the overall surgical discrepancy for these landmarks. The same principle was applied to define other parameters, including L3, L6, L7, and No.

Table 3 Perioperative and postoperative outcomes in Group A and Group B

Parameter	Group A (n=30)	Group B (n=30)	*P*
Operative time (min)	235.5 ± 28.6	218.3 ± 25.1	0.38
Estimated blood loss (ml)	285.4 ± 62.3	272.5 ± 58.7	0.42
Navigation registration attempts >1	2 (6.7%)	-	-
Navigation system failure	0 (0%)	-	-
Transient mental nerve hypoesthesia	0 (0%)	1 (3.3%)	0.31
Persistent inferior alveolar nerve injury	0 (0%)	0 (0%)	-
Hardware complication	0 (0%)	0 (0%)	-
Postoperative infection	0 (0%)	0 (0%)	-
Revision surgery	0 (0%)	0 (0%)	-

Data are presented as mean±standard deviation or n (%). *P*-values were calculated using independent t-test for continuous variables and Fisher's exact test for categorical variables.

Figures

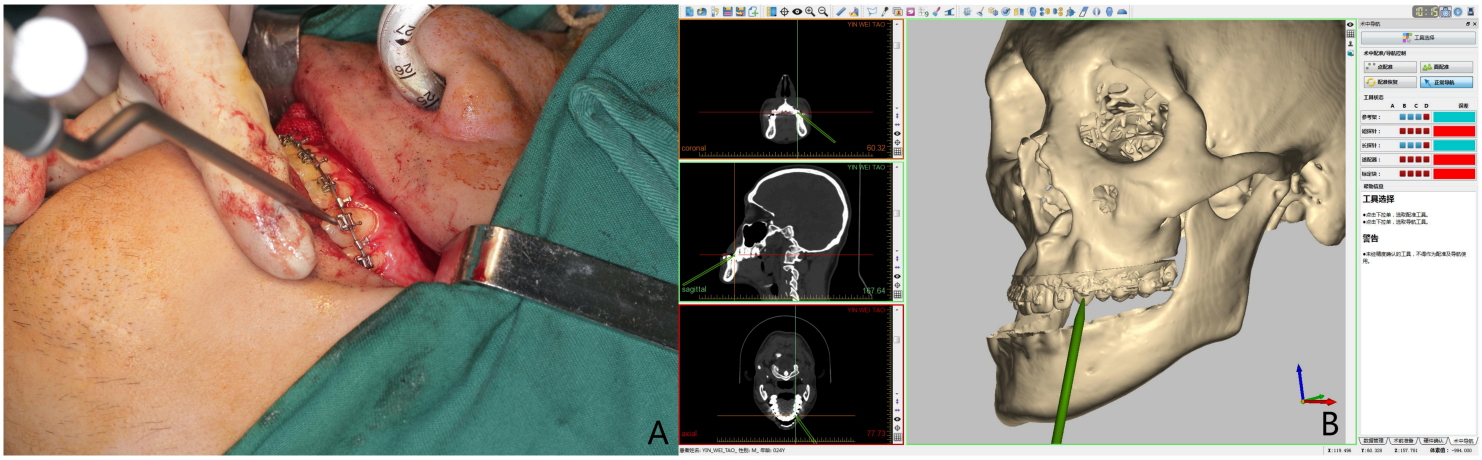


Figure 1

Legend not included with this version.

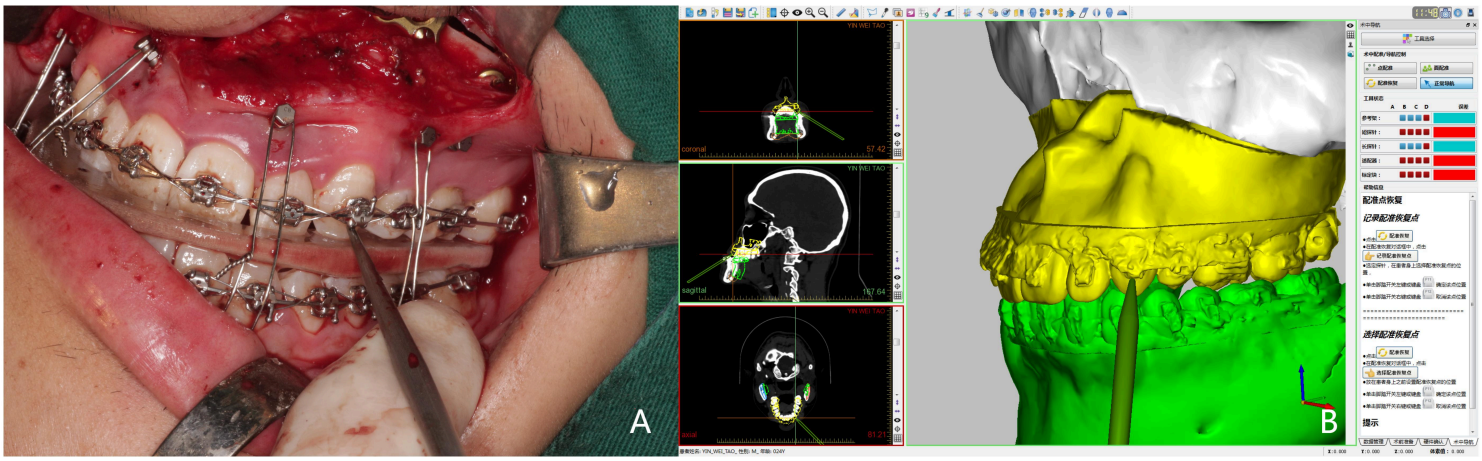


Figure 2

Legend not included with this version.

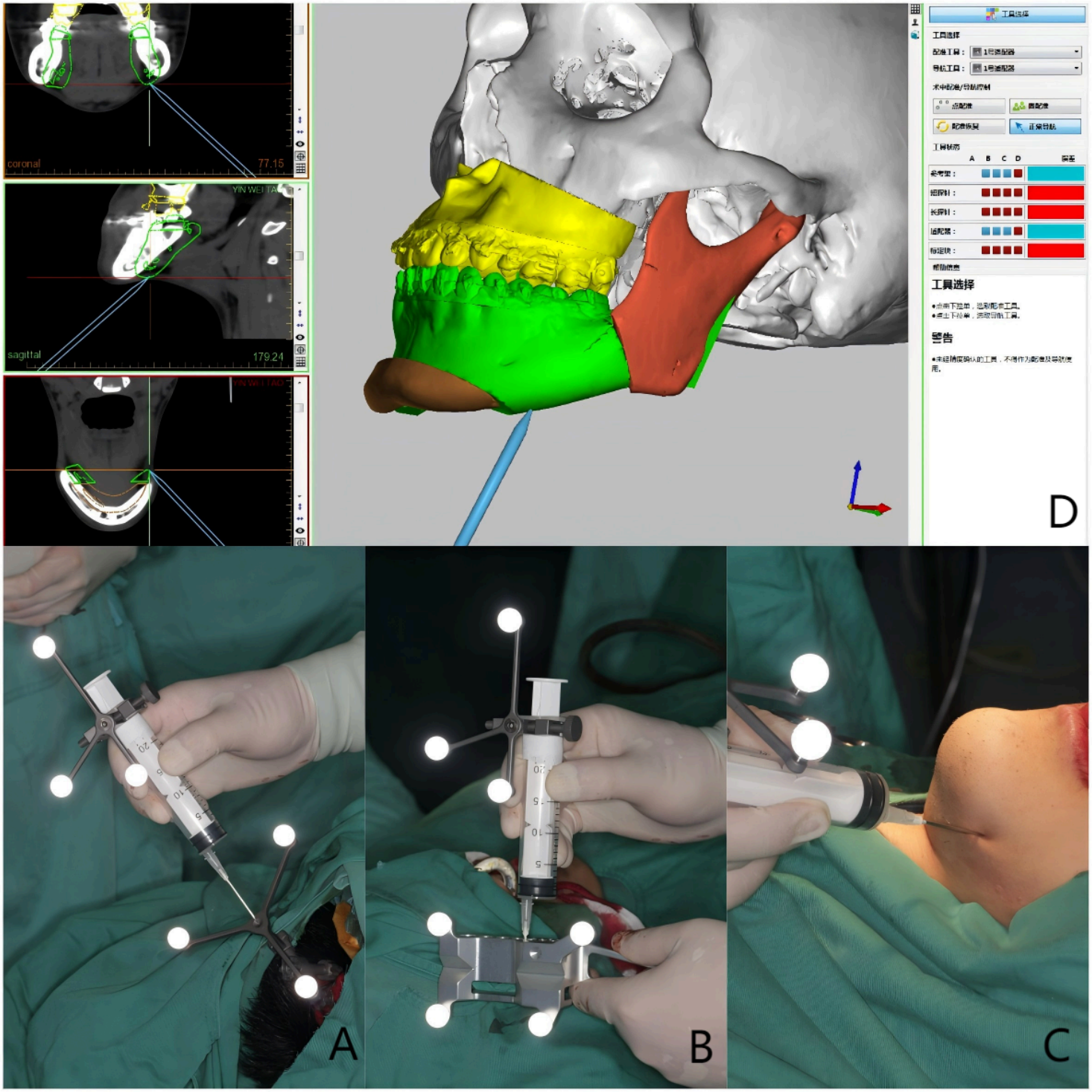


Figure 3

Legend not included with this version.

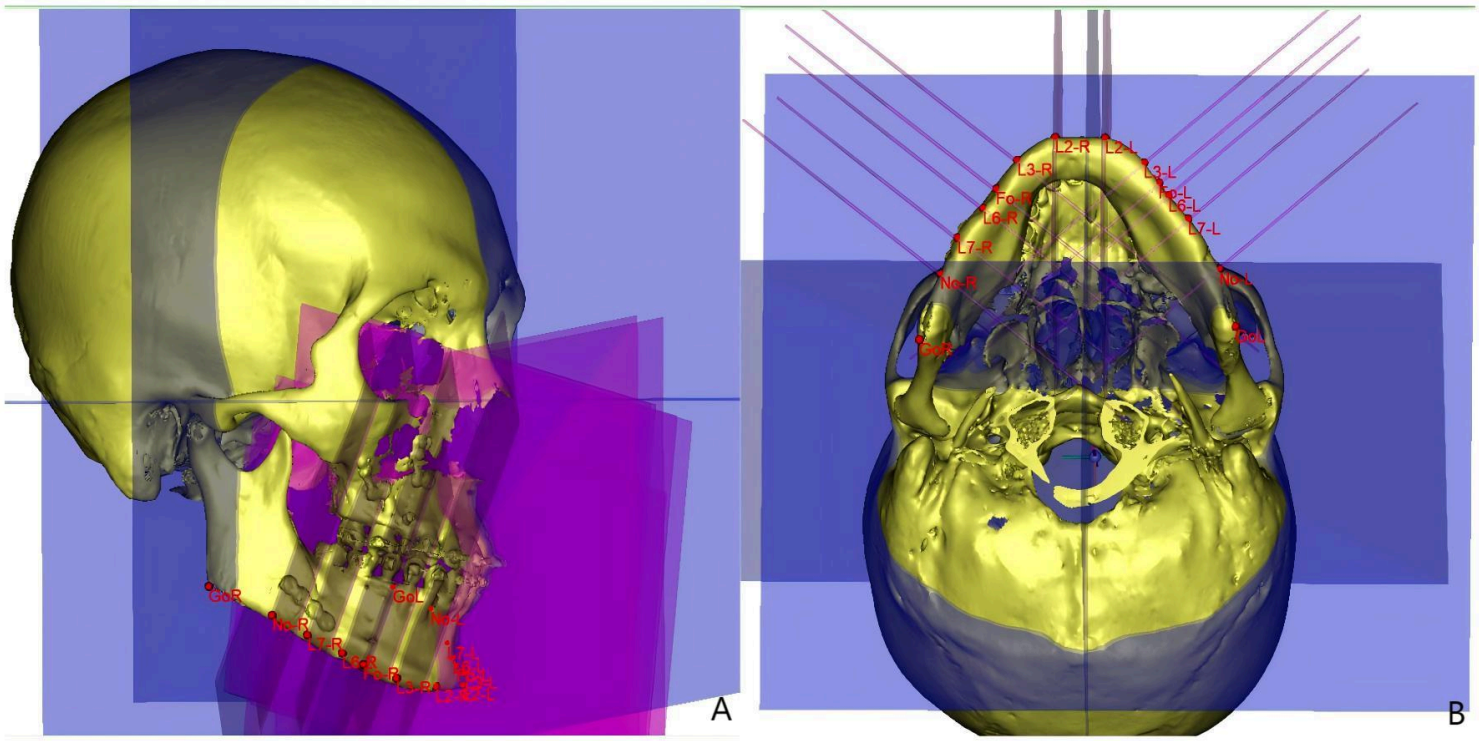


Figure 4

Legend not included with this version.

Supplementary Files

This is a list of supplementary files associated with this preprint. Click to download.

- STROBECHECKLIST.pdf